ISSN 0016-8521, Geotectonics, 2018, Vol. 52, No. 2, pp. 225–239. © Pleiades Publishing, Inc., 2018.
Original Russian Text © M.Yu. Kurapov, V.B. Ershova, A.A. Makariev, E.V. Makarieva, A.K. Khudoley, M.V. Luchitskaya, A.V. Prokopiev, 2018, published in Geotektonika, 2018, No. 2, pp. 76–90.

Carboniferous Granitoid Magmatism of Northern Taimyr: Results of Isotopic-Geochemical Study and Geodynamic Interpretation

M. Yu. Kurapov[a], *, V. B. Ershova[a], A. A. Makariev[b], E. V. Makarieva[b], A. K. Khudoley[a], M. V. Luchitskaya[c], and A. V. Prokopiev[d]

[a]*Geological Faculty, St. Petersburg State University, St. Petersburg, 199034 Russia*
[b]*Polar Marine Geosurvey Expedition, St. Petersburg, 198412 Russia*
[c]*Geological Institute, Russian Academy of Sciences, Moscow, 109017 Russia*
[d]*Diamond and Precious Metal Geology Institute, Siberian Branch, Russian Academy of Sciences, Yakutsk, 677077 Russia*
**e-mail: mikhail.kurapov@gmail.com*

Received August 14, 2017

Abstract—Data on the petrography, geochemistry, and isotopic geochronology of granites from the northern part of the Taimyr Peninsula are considered. The Early–Middle Carboniferous age of these rocks has been established (U–Pb, SIMS). Judging by the results of $^{40}Ar/^{39}Ar$ dating, the rocks underwent metamorphism in the Middle Permian. In geochemical and isotopic composition, the granitic rocks have much in common with evolved I-type granites. This makes it possible to specify a suprasubduction marginal continental formation setting. The existence of an active Carboniferous margin along the southern edge of the Kara Block (in present-day coordinates) corroborates the close relationship of the studied region with the continent of Baltia.

Keywords: Taimyr, syncollisional granites, Permian metamorphism, active margin, I-type granite
DOI: 10.1134/S0016852118020048

INTRODUCTION

The Taimyr–Severnaya Zemlya Fold Region is situated north of Siberian Platform and comprises the Taimyr Peninsula, Severnaya Zemlya Archipelago, and the adjoining shelf of the Kara Sea. This region is subdivided into the southern, central, and northern tectonic zones [2]. The studied granitoids are localized in the Northern Taimyr Zone, which covers the northern part of the Taimyr Peninsula and islands of the Severnaya Zemlya Archipelago. Various authors refer this region the southern part of the so-called Kara Block (Terrane) or the North Kara Terrane [2, 28, 33], most of which is hidden under the waters of the Kara Sea. Its suggested boundaries have largely been traced using geophysical data [6]. Only the southern part of the Kara Block is accessible for its direct study. It is separated from the Central Taimyr Zone, which is apparently a continuation of the Siberian continent in the Paleozoic, by the Main Taimyr and Diabasic faults [2] (Fig. 1).

The geodynamic position and geological history of the Kara Block has remained a matter of debate until now. Several geodynamic models describing the tectonic nature and arrangement of this region in the Phanerozoic have been proposed. According to [8], the Kara block is a constituent of the ancient Arctida paleocontinent [28]; in model [28], the North-Kara Terrane was a part of the continent of Baltia. In model [33], the Paleozoic Kara Block is regarded as a separate terrane. Such significant divergences in notions of researchers have been caused by heterogeneous geological data [8], paleomagnetic data [33], and dating of clastic zircons [28]. A substantial drawback of earlier proposed models is the poor knowledge of Late Paleozoic magmatism within the Kara Block, which has been considered only by Vernikovsky [2, 3]. The aim of our paper is to fill this gap, at least partly, by determining the age of the oldest syncollision granitoids from the Northern Taimyr, as well as carrying out comprehensive petrographic, geochemical, and isotopic-geochemical characterization to establish the geodynamic nature of the granitoids and refine the Kara Block evolution models.

GEOLOGY

The granitic massifs considered in this paper occur in the Northern Taimyr Zone. Upper Vendian (?) and Cambrian rocks mainly occur in this zone. Jurassic and Cretaceous rocks are less abundant.

Upper Vendian (?) and Cambrian rocks are widespread in the western part of the territory. They are commonly represented by rhythmically intercalating sandstone, siltstone, and claystone that metamor-

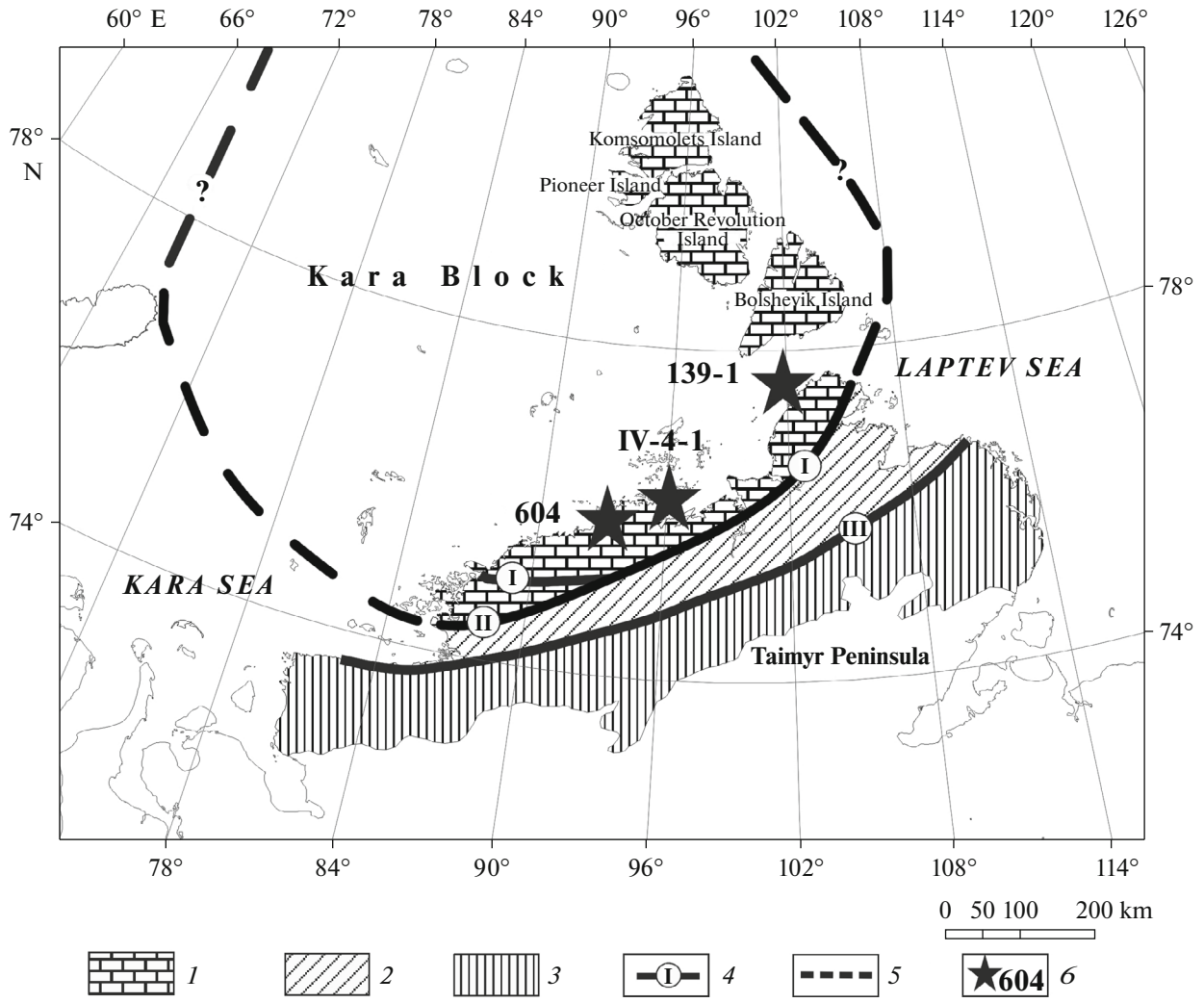

Fig. 1. Location of studied region and localization of samples. Arbitrary notes: (*1*) Northern Taimyr Tectonic Zone, (*2*) Central Taimyr Tectonic Zone, (*3*) Southern Taimyr Tectonic Zone, (*4*) faults (numerals in circles): I, Main Taimyr; II, Diabasic, III, Pyasina–Fadeevsky; (*5*) inferred boundaries of Kara Block; (*6*) studied massif.

phosed under conditions up to amphibolite facies; earlier they were called Riphean [2, 4]. They are overlapped by Jurassic–Cretaceous sequences with a sharp angular unconformity. The latter are slightly lithified clastic rocks with coal lenses and layers. Lenses of organogenic limestone locally occur in the lower part of the section [4].

The Paleozoic granitic rocks are widespread in the North Taimyr Zone. They are exposed as relatively small intrusive bodies cutting through Upper Vendian (?)–Paleozoic metasedimentary complexes. The results of geochronological study of biotite and biotite–amphibole granitoids [2] were obtained on the Northern Taimyr near the coast of Khariton Laptev (Cape Kaminsky). U–Pb dating of monazite from the granitoids yields a concordant age of 306 ± 2 Ma. The Rb–Sr age (277 ± 4 Ma) of the same granitoids was interpreted as the time of metamorphism. Granitoids from the northeastern Taimyr (Cape Chelyuskina), which cut through the fold structure and was not affected by metamorphism, show an Early Permian age. U–Pb dating of zircon yielded 264 ± 8 Ma for the upper intersection of concordia and discordia and 252 ± 1 Ma for biotite with the $^{40}Ar/^{39}Ar$ method [2, 3].

RESEARCH METHODS

The U–Pb dating of zircons was carried out with a SHRIMP-II ion microscope at the Center of Isotopic Research, Russian Geological Research Institute (VSEGEI), St. Petersburg. Separation of zircon monofractions was performed according to the standard scheme: comminution, a screen grader, the <0.25 mm fraction was passed through a centrifugal concentrator, and the obtained heavy fraction was processed with an electromagnet. The concentrate

was finished in a heavy liquid. The selected zircon grains were implanted in an epoxy resin together with the standard TEMORA and 91500 grains. They were ground and polished to approximately half their thickness. To choose the dating points, cathodoluminescent images reflecting the internal structure and zoning of zircon were used. The U/Pb ratios were measured on the SHRIMP-II according to the technique described in [40]. The intensity of the primary beam of negatively charged molecular oxygen ions was 2.5–4.0 nA, and the spot (crater) diameter was 15 × 10 μm.

The data were processed in the SQUID program [29]. The U/Pb ratios were normalized to 0.0668, i.e., to the value assigned to the standard TEMORA zircon, corresponding to an age of 416.75 Ma [17]. Uncertainties in single analyses (ratios and ages) were brought to conformity at a level of ±1σ and uncertainties in calculated concordant ages, at a level of ±2σ. The ISOPLOT program was used to construct graphs with concordia [30].

Dating by the $^{40}Ar/^{39}Ar$ method was performed at the Sobolev Institute of Geology and Mineralogy, Siberian Branch, Russian Academy of Sciences, in Novosibirsk. The measurement technique is described in [15]. Charges of mineral fractions were wrapped in aluminum foil. After spilling, they were soldered in a quartz ampoule together with MCA-11 and LP-6 biotite charges as monitors. Afterward, the fractions were irradiated in the cadmium-plated channel of a VVR-K scientific reactor at the Research Institute of Nuclear Physics. The gradient of the neutron flux did not exceed 0.5% of the sample size. Experimental stepwise heating was carried out in a quartz reactor with an externally heated oven. A blank run with ^{40}Ar (10 min at 12000°C) did not exceed 5×10^{-10} ncm^3. Purification of argon was carried out with ZrAl SAES getters. The isotopic composition of argon was measured on a Noblegas 5400 mass spectrometer (Micromass, England). Measurement errors in the text and figures correspond to ±1σ.

The isotopic composition of Sr was determined at the Institute of Precambrian Geology and Geochronology, RAS. Rb and Sr were separated by a technology close to that described in [14]. The isotopic compositions of Rb and Sr were measured on a TRITON TI multicollector mass spectrometer in the static regime. The measurement accuracy was ±0.5% for Rb and Sr, 0.05% for $^{87}Rb/^{86}Sr$, and 0.007% for $^{87}Sr/^{86}Sr$ (2σ). Taking into account the correction to instrumental fractionation ($^{88}Sr/^{86}Sr = 8.37521$), the weight average $^{87}Rb/^{86}Sr$ of Sr in standard BCR-1 over the measurement period is 0.710241 ± 0.000015 (2σ, $n = 10$). The level of the blank run over the study period is 0.05–0.15 ng for Rb and 0.1–0.5 ng for Sr.

Geochemical studies were carried out at the Central Laboratory of VSEGEI, St. Petersburg. The contents of major oxides were determined on an ARL 9800 XRF spectrometer. The contents of minor elements (including REE) were determined on an OPTIMA 4300DV emission spectrometer and an ELAN 6100 DRC mass spectrometer.

PETROGRAPHY

Sample 139-1 was taken from one of the Geiberg Islands north of Taimyr Peninsula (Fig. 1). The intrusive massif is represented by coarse-grained porphyry-like muscovite–biotite granite. Relationships with the host rocks were established. The granite is characterized by a trachytoid texture and porphyry-like structure. The former is expressed in a near-parallel arrangement of K-feldspar crystals. Granite is composed of quartz (25%), plagioclase (40%), microcline (20%), biotite (20%), muscovite (5%) (Fig. 2a). Isometric quartz crystals are 1–5 mm in size. Plagioclase (An_{20}) is represented by tabular crystals 3–7 mm in size with thin polysynthetic twinning. Microcline is represented by tabular crystals with a lattice structure 3–6 mm in size. Biotite laths are 1–5 mm in size, while muscovite tablets and small flakes are 0.5 to 3.0 mm in size. Accessory zircon has been noted.

Sample 604 was taken from the granitic massif exposed along the Volchii Bay in the central part of the Northern Taimyr. The massif cuts through Upper Vendian (?) rocks (Fig. 1). The intrusive rocks are represented by medium-grained biotite–muscovite leucogranite. Its texture is gneisslike and its structure is granitic (hypidiomorphic-granular). The rock consists of quartz (30%), plagioclase (30%), microcline (20%), biotite (5%), and muscovite (15%) (Fig. 2b). Isometric quartz crystals are 0.5–2 mm in size. Plagioclase (An_{15}) is represented by tabular crystals with thin polysynthetic twinning. Heterogeneous block extinction and nonuniform twinning of crystals are observed. Microcline is represented by tabular crystals 2.5 to 5.0 mm in size. Biotite and muscovite laths are 0.2–5.0 and 0.1–6.0 mm in size, respectively. Accessory minerals are represented by apatite and zircon.

Sample IV-4-1 was taken from the granitic massif on the Cape Yeremeeva in central part of the Northern Taimyr. The massif cuts through metamorphosed Cambrian rocks (Fig. 1). The intrusive rock is represented by fine- to medium-grained biotite–muscovite leucogranite in composition. Texture is massive and structure is granitic. The rock consists of quartz (40%), plagioclase (40%), microcline (5%), biotite (5%), and muscovite (15%) (Fig. 2c). Isometric quartz crystals are 0.5–2.0 mm in size (0.8 mm is a predominant size). Plagioclase ($An_{15–20}$) is represented by tabular and prismatic crystals with thin polysynthetic twinning (0.6–1.5 mm) and zonal structure. Tabular microcline crystals vary from 0.3 to 1.0 mm in size. Biotite is represented by flakes and tablets 0.3–1.2 mm in size; muscovite laths are 0.6–1.5 mm in dimensions. Apatite, zircon, and magnetite are accessory minerals.

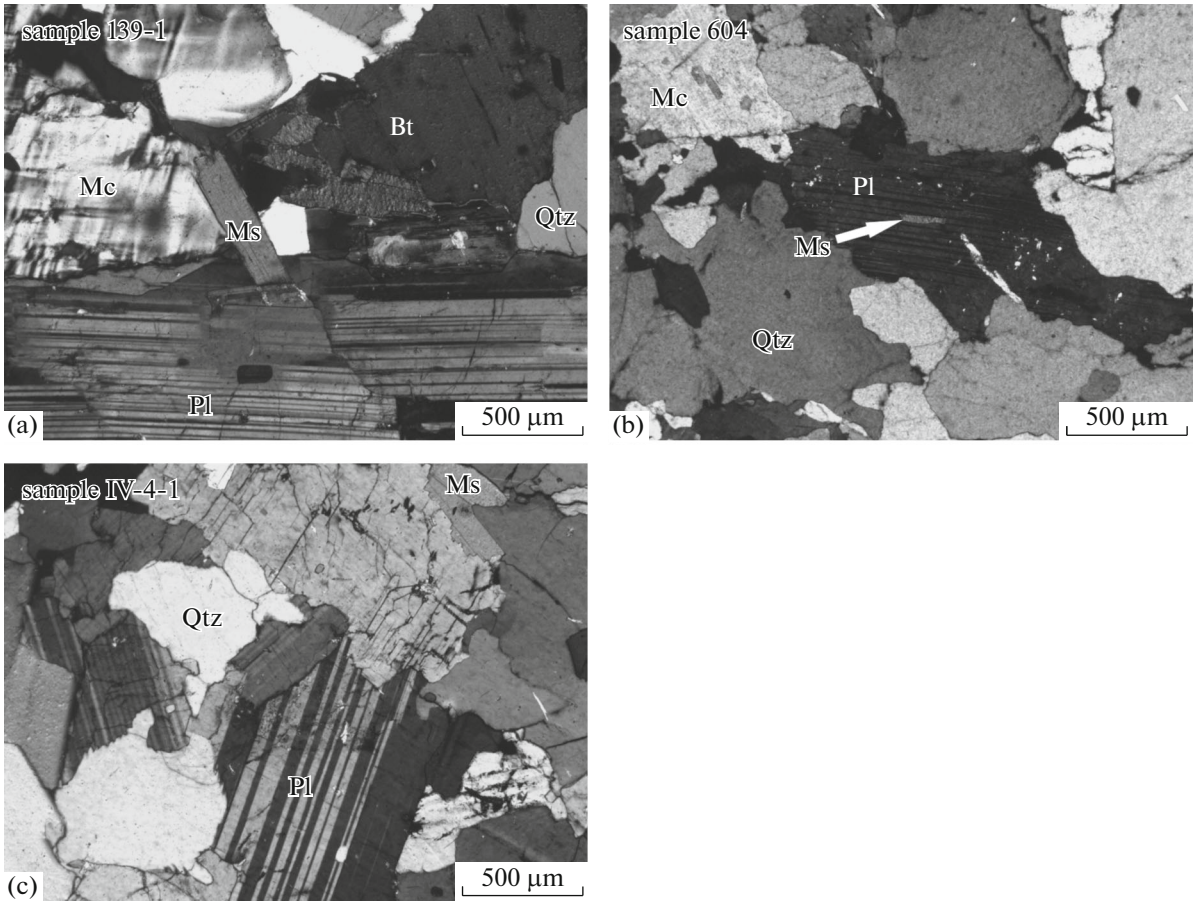

Fig. 2. Photomicrographs of thin section of granitic rocks, crossed polars: (a) coarse-grained porphyry-like muscovite–biotite granite (sample 139-1); (b) medium-grained biotite–muscovite granite (sample 604); (c) fine- to medium-grained biotite–muscovite granite (sample IV-4-1).

GEOCHRONOLOGY

Coarse-Grained Two-Mica Granite (Sample 139-1)

Figure 3 shows photomicrographs of the dated zircon crystals (10 grains) exposed in the cathodoluminescence regime. Zircons are up to 600 μm in size, perfect in crystallographic forms, and have fine zoning typical of magmatic minerals. Dark and poorly transparent crystals are enriched in uranium (up to 1881 g/t, see Table 1). The Th/U ratio varies from 0.09 to 0.72, apparently recording younger hydrothermal alteration and possible disturbance of the U–Pb isotopic system. Nevertheless, U–Pb dating of nine zircon grains yielded a concordant age of 315 ± 1 Ma (Fig. 4). Another grain (Table 1, grain 2.1) has a $^{206}Pb/^{238}U$ age of 287 ± 3 Ma. Precisely this grain is characterized by the highest U and Th contents: 1881 and 992 g/t, respectively, so that the obtained isotopic age hardly corresponds to magmatic activity. This sample reveals a distinct plateau in the ^{40}Ar–^{39}Ar system corresponding to 90% of separated ^{39}Ar; its age is 318 ± 3 Ma (Fig. 5, Table 2).

Medium-Grained Two-Mica Leucogranite (Sample 604)

Ten grains have been dated; their cathodoluminescent images are shown in Fig. 3. The grain sizes are 150–250 μm; their morphology is variable. In one of the grains, an overgrowth structure is clearly seen, and this grain has been dated separately at two points in the central part and the outer rim. The U and Th contents vary widely (from 225 to 2024 and from 2 to 337 g/t, respectively), providing evidence for intense secondary alterations. This is also supported by a widely varying Th/U ratio from 0.003 to 0.49. The high discordance in five of the ten grains is also a result of secondary alteration, so that these grains cannot be involved in determining the isotopic age of rocks (Table 1). Four datings are close to the concordant values; three (2.1, 4.1, 5.1) make up a cluster with a concordant age of 345 ± 4 Ma (Fig. 4). These grains are distinguished by extremely low Th/U ratios (0.003, 0.09, 0.01), and the inherited isotopic age apparently does not fit the main magmatic event [25]. In support of such an interpretation, the central part of grain 4.2 is characterized by an older age (563 ± 7 Ma), which is also close to

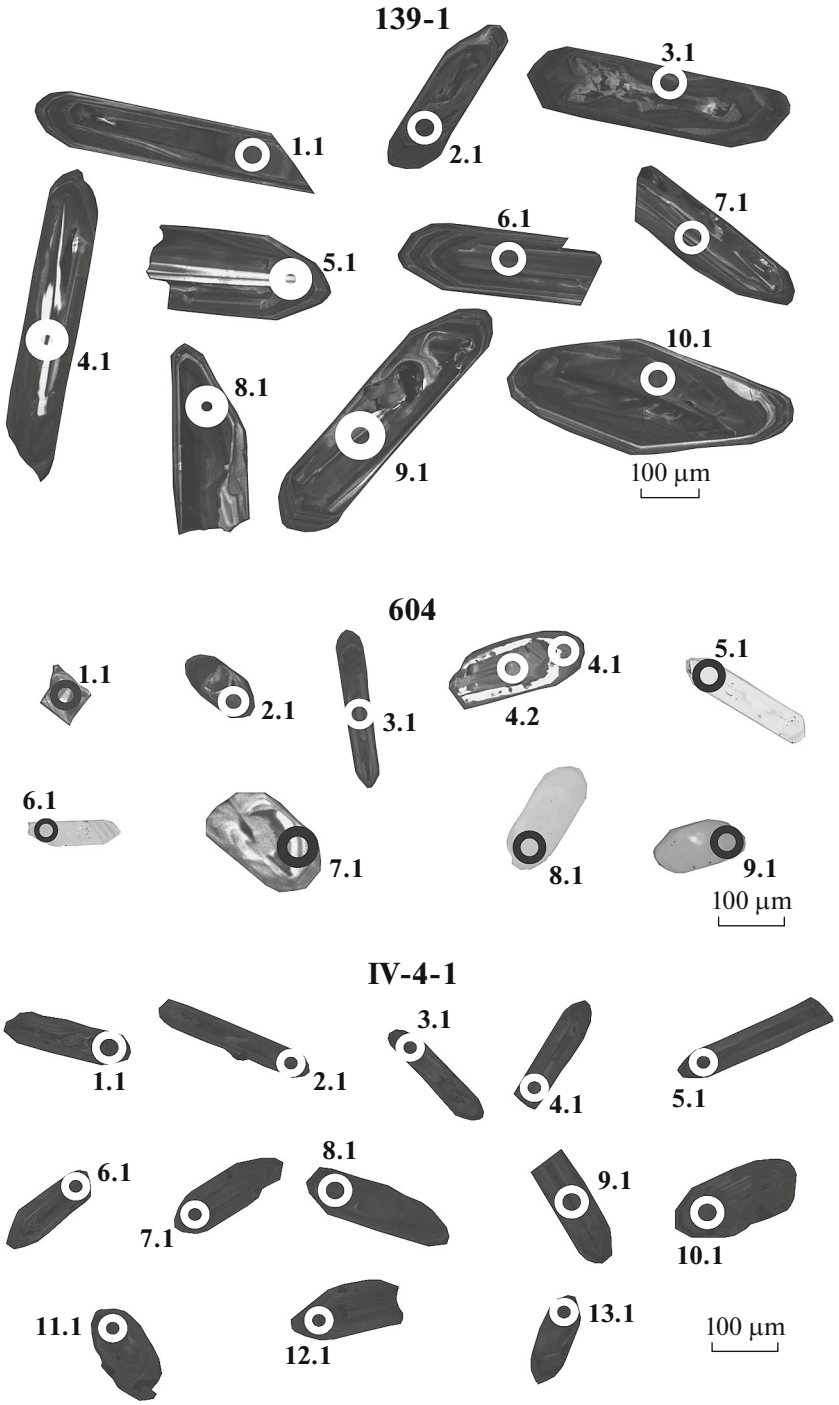

Fig. 3. Photomicrographs of zircons in cathodoluminescence regime. Numerals are sample numbers.

concordant value. A lack of indications of metamorphic influence makes it possible to suggest that anomalous geochemistry of zircons are related to crystallization of them from a residual melt coeval with intense hydrothermal activity. Thus, the result obtained corresponds to the latest phase of magmatic activity during formation of granite intrusion. At dating of muscovite with $^{40}Ar/^{39}Ar$ method, a distinct plateau is observed in sample spectrum. It is corresponds to 99.6% of separated ^{39}Ar and to age of 270 ± 3 Ma (Fig. 5; Table 2). Grain 1.1 with a moderate discordance yielded an age of 245 ± 4 Ma.

Fine- to Medium-Grained Two-Mica Leucogranite (Sample IV-4-1)

Thirteen grains were selected for dating (Fig. 3). All of them were 150–300 μm in size with perfect crystal-

Table 1. Results of U–Pb dating of zircons

Grains and points	Contents of elements					Age, Ma				Isotope ratios						
	% $^{206}Pb_c$	U, g/t	Th, g/t	$^{232}Th/^{238}U$	$^{206}Pb^*$, g/t	(1) $^{206}Pb/^{238}U$ Age		(1) $^{207}Pb/^{206}Pb$ Age		(1) $^{207}Pb/^{206}Pb$	±%	(1) $^{207}Pb^*/^{235}U$	±%	(1) $^{206}Pb^*/^{238}U$	±%	Correlation of errors
IV-4-1																
1.1	8.25	2001	152	0.08	106	354.7	±5.5	160	±410	0.1162	1.2	0.384	17	0.0566	1.6	0.09
2.1	16.08	2158	183	0.09	144	407.4	±8.1	684	±500	0.1911	3.7	0.56	24	0.0652	2	0.087
3.1	5.68	2431	274	0.12	109	310.8	±5.1	722	±560	0.108	13	0.43	27	0.0494	1.7	0.063
4.1	6.37	1137	107	0.10	41.1	249.2	±5.1	346	±510	0.1043	5.1	0.29	23	0.0394	2.1	0.091
5.1	11.21	2741	468	0.18	141	334	±5.1	132	±410	0.1395	1.4	0.357	17	0.0532	1.6	0.090
6.1	10.33	1949	186	0.10	89.4	301.5	±5.1	122	±490	0.1319	1.6	0.32	21	0.0479	1.7	0.083
7.1	12.59	2087	241	0.12	122	372.2	±6.3	−200	±610	0.1455	1.1	0.348	24	0.0594	1.7	0.072
8.1	14.71	2234	243	0.11	129	357.8	±6	533	±630	0.176	6.6	0.46	29	0.0571	1.7	0.059
9.1	17.41	1796	343	0.20	98.5	331.1	±6.7	−230	±820	0.184	1.1	0.305	33	0.0527	2.1	0.063
10.1	0.56	1788	185	0.11	79.6	324.1	±4.1	224	±100	0.0551	1.9	0.36	4.7	0.0516	1.3	0.278
11.1	0.39	2097	205	0.10	91.9	319.4	±4	250	±73	0.0543	1.8	0.359	3.4	0.0508	1.3	0.374
12.1	5.73	2118	3916	1.91	125	402.9	±5.8	381	±270	0.1006	1.4	0.482	12	0.0645	1.5	0.123
13.1	1.34	1535	147	0.10	67.3	316.7	±4.4	253	±180	0.0621	2	0.356	8.1	0.0504	1.4	0.176
139-1																
2.1	2.77	1881	992	0.55	73.5	287	±2.9	272	±110	0.0517	4.8	0.324	4.9	0.0455	1.0	0.208
1.1	0.00	720	61	0.09	30.9	314	±3.4	337	±32	0.0532	1.4	0.366	1.8	0.0499	1.1	0.608
3.1	0.37	1353	335	0.26	58.3	316	±3.1	317	±43	0.0527	1.9	0.365	2.2	0.0502	1.0	0.466
4.1	4.32	321	225	0.72	13.9	316	±4.2	549	±243	0.0585	11.1	0.406	11.2	0.0503	1.4	0.122
5.1	0.54	387	124	0.33	16.6	314	±3.4	258	±98	0.0514	4.3	0.353	4.4	0.0499	1.1	0.252
6.1	0.31	707	409	0.60	30.3	314	±3.2	317	±58	0.0527	2.6	0.363	2.8	0.0499	1.0	0.380
7.1	1.38	773	372	0.50	33.4	316	±3.3	339	±104	0.0532	4.6	0.369	4.7	0.0502	1.1	0.227
8.1	1.02	1065	164	0.16	45.7	314	±3.2	416	±74	0.0551	3.3	0.380	3.5	0.0500	1.0	0.299
9.1	0.75	601	396	0.68	26	317	±3.4	285	±93	0.0520	4.1	0.362	4.2	0.0504	1.1	0.257
10.1	0.53	1039	514	0.51	44.7	315	±3.2	321	±60	0.0528	2.6	0.365	2.8	0.0501	1.0	0.363
604																
1.1	0.00	305	146	0.49	10.1	244.6	±3.6	175	±110	0.0496	4.7	0.264	5	0.03868	1.5	0.300
2.1	0.22	838	74	0.09	39.5	343.8	±3.6	368	±70	0.0539	3.1	0.407	3.3	0.05477	1.1	0.330
3.1	2.16	1751	374	0.22	118	474.8	±4.6	3109	±28	0.2381	1.7	2.511	2	0.07644	1	0.502
4.1	0.24	678	2	0.003	33	354.3	±3.9	361	±77	0.0537	3.4	0.419	3.6	0.0565	1.1	0.316
4.2	0.34	400	61	0.16	31.5	563.1	±6.6	551	±89	0.0586	4.1	0.737	4.3	0.0913	1.2	0.287
5.1	0.14	1208	116	0.10	55.9	337.7	±3.4	323	±56	0.0529	2.5	0.392	2.7	0.05379	1	0.389
6.1	1.10	2024	337	0.17	190	662.2	±6.2	2174	±29	0.1358	1.7	2.026	1.9	0.1082	0.98	0.504
7.1	0.00	683	269	0.41	20.1	217.3	±4.2	1740	± 6	0.1065	4.1	0.503	4.6	0.03429	2	0.432
8.1	0.00	225	18	0.08	14.4	462.8	±6.8	2603	±42	0.1747	2.5	1.793	2.9	0.0744	1.5	0.516
9.1	0.33	1515	11	0.01	103	487.5	±4.5	2660	±25	0.1808	1.5	1.958	1.8	0.07856	0.96	0.533

(1) means correction for common lead based on measured ^{204}Pb contents. Pb_c and Pb* are contents of common and radiogenic lead, respectively.

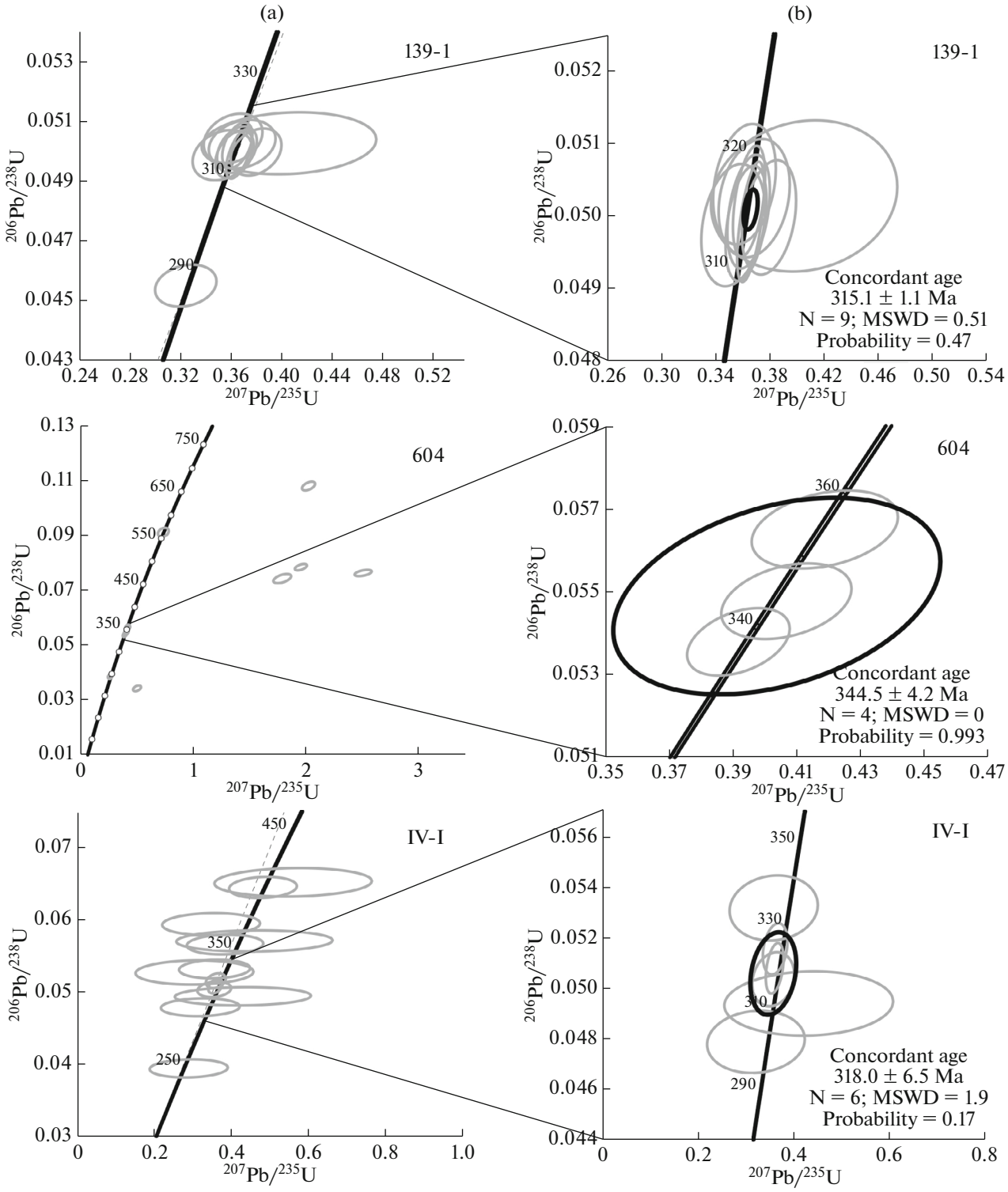

Fig. 4. Diagrams with concordia for granitoids of Northern Taimyr. (a) All dated grains; (b) grains used to calculate concordia.

lographic shape. The internal structure of grains is poorly seen because of insufficient transparence and dark color caused by a high uranium content (1137–2741 g/t). In grain 12.1, Th/U = 1.91, however, high concentrations of U and Th (2118 and 3916 g/t, correspondingly) provide evidence for the possible influence of younger secondary processes and disturbance of the U–Pb isotopic system. The Th/U ratio in most grains is close to 0.10–0.11, and these values are markedly lower than in typical magmatic grains [25]. The

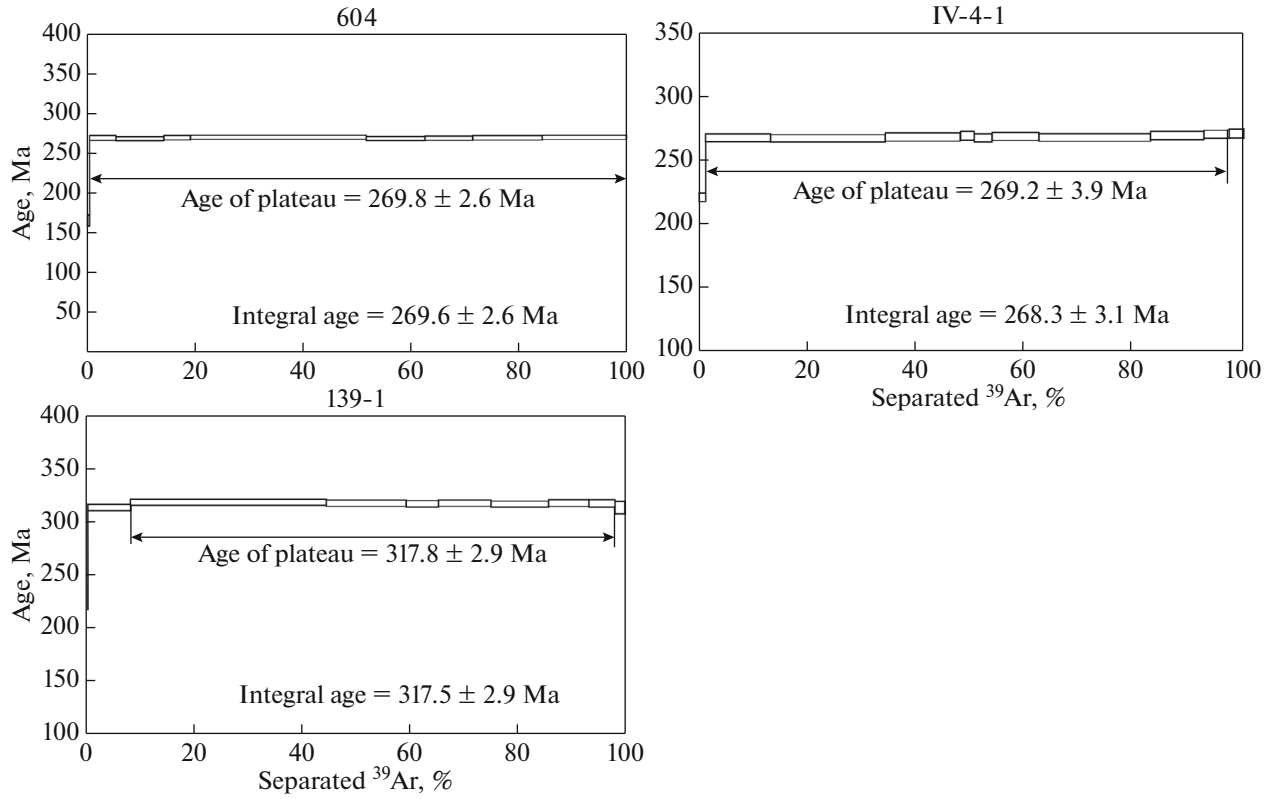

Fig. 5. Results of $^{40}Ar/^{39}Ar$ dating of micas from granitic rocks. Numerals are sample numbers.

high uranium concentrations confirm that these grains were intensely affected by secondary processes or they crystallized from residual melts, recording the last crystallization phases. The presence of a cluster of six grains with a concordant age of 318 ±7 Ma suggests that their formation is related to crystallization from residual melts. An additional five grains close in morphology and geochemistry contain relics of older melt crystallization phases (Fig. 4). A grain with Th/U = 1.91 had an older $^{206}Pb/^{238}U$ age (403 ± 6 Ma). In the case of biotite dating by the $^{40}Ar/^{39}Ar$ method, the spectrum of the sample includes a distinct plateau corresponding to 95.9% of separated ^{39}Ar and to an age of 269 ± 3 Ma (Fig. 5; Table 2). A close $^{206}Pb/^{238}U$ age was also established for the youngest grain 4.1 (249 ± 5 Ma).

PETROGEOCHEMICAL FEATURES

The studied Carboniferous granitoids contain 68–73 wt % SiO_2 (Table 3). The rocks are reffered to calc-alkaline and high-potassic series by the ratio of K_2O and SiO_2, as well as to subalkaline granite and leucogranite by the ratio of total alkali and silica contents. According to the classification by Frost et al. [21], the granitoids are related to magnesian (Fe* = $FeO_{tot}/(FeO_{tot} + MgO) = 0.59–0.73$), and alkali–calc and calc–alkaline peraluminous (ASI > 1.1) rocks. The magnesian composition of granitoids makes it possible to compare them with I-type granites, while the high ASI index characteristic of all samples brings them closer to with peraluminous S-type granites.

Granite (sample 139-1) and leucogranite (sample IV-4-1) are characterized by high total REE contents (300 and 311 g/t, respectively). Leucogranite (sample 604) differs by a lower total REE content (82 g/t).

Granite and leucogranite are characterized by a fractionated REE distribution enriched in LREE and depleted in HREE ($La_N/Yb_N = 18.34–42.19$) (Fig. 6a). All rocks are distinguished by a variously expressed negative Eu anomaly (Eu/Eu* = 0.21–0.51). Spider diagrams of granitoids are characterized by a similar distribution of LILE with respect to HFSE and the minima of Ba, Nb, Sr, and Ti contents (Fig. 6b), inherent to suprasubduction igneous rocks.

The studied granitoids were compared to granites of various other petrochemical types using a series of diagrams with plotted both major and minor chemical elements. In the Nb–Sr plot (Fig. 7a) [39], the data points of granitoids are clustered around the mean value of I-type granites, whereas in the P_2O_5–SiO_2 and Rb–Y plots, they follow the trend of S-type granites (Figs. 7b, 7c) [18]. In the $Fe_2O_3 \cdot 5$–$Na_2O + K_2O$–

Table 2. Results of $^{40}Ar/^{39}Ar$ dating

T, °C	t, min	^{40}Ar(STP)	$^{40}Ar/^{39}Ar$	±1σ	$^{38}Ar/^{39}Ar$	±1σ	$^{37}Ar/^{39}Ar$	±1σ	$^{36}Ar/^{39}Ar$	±1σ	Ca/K	$\Sigma^{39}Ar$, %	Age, Ma	±1σ
Muscovite 604, charge 44.28 mg, $J = 0.003959 \pm 0.000041$*; integral age = 269.6 ± 2.6 Ma; age of plateau (650–1130°C) = 269.8 ± 2.6 Ma														
500	10	$8.5e^{-9}$	42.943	0.383	0.03624	0.00726	0.211	0.030	0.06314	0.00339	0.761	0.4	165.6	6.8
650	10	$109.0e^{-9}$	42.658	0.021	0.02017	0.00081	0.022	0.010	0.00642	0.00065	0.080	5.2	269.9	2.9
725	10	$195.2e^{-9}$	41.766	0.020	0.01998	0.00036	0.022	0.003	0.00399	0.00012	0.078	14.1	268.8	2.6
775	10	$110.8e^{-9}$	42.877	0.018	0.01953	0.00073	0.029	0.012	0.00702	0.00053	0.104	19.1	270.2	2.8
850	10	$721.2e^{-9}$	42.039	0.007	0.01918	0.00008	0.005	0.002	0.00391	0.00006	0.017	51.7	270.7	2.6
900	10	$235.3e^{-9}$	41.273	0.015	0.01992	0.00032	0.006	0.004	0.00224	0.00021	0.020	62.5	269.0	2.6
975	10	$194.2e^{-9}$	41.472	0.015	0.01957	0.00026	0.009	0.003	0.00264	0.00019	0.031	71.5	269.5	2.6
1050	10	$281.2e^{-9}$	41.453	0.011	0.01925	0.00022	0.004	0.004	0.00241	0.00019	0.015	84.4	269.8	2.6
1130	10	$340.0e^{-9}$	41.390	0.007	0.01867	0.00007	0.006	0.004	0.00175	0.00017	0.023	100.0	270.6	2.6
Biotite 139-1, charge 24.82 mg, $J = 0.003859 \pm 0.000039$*; integral age = 317.5 ± 2.9 Ma; age of plateau (700–1100°C) = 317.8 ± 2.9 Ma														
500	10	$5.9e^{-9}$	73.059	1.215	0.06744	0.00526	0.150	1.026	0.12815	0.00643	0.542	0.2	229.7	11.8
600	10	$146.0e^{-9}$	55.689	0.036	0.02264	0.00031	0.002	0.028	0.02177	0.00013	0.007	8.2	313.9	2.9
700	10	$609.7e^{-9}$	50.733	0.009	0.01857	0.00014	0.003	0.009	0.00212	0.00009	0.012	44.6	318.9	3.0
750	10	$248.4e^{-9}$	50.710	0.020	0.01917	0.00014	0.002	0.020	0.00266	0.00031	0.008	59.4	317.8	3.0
800	10	$102.3e^{-9}$	51.968	0.032	0.01837	0.00042	0.004	0.053	0.00717	0.00008	0.015	65.4	317.4	3.0
900	10	$168.9e^{-9}$	52.201	0.036	0.01972	0.00027	0.026	0.040	0.00763	0.00049	0.093	75.2	318.0	3.1
1000	10	$182.3e^{-9}$	51.697	0.015	0.02041	0.00029	0.076	0.020	0.00652	0.00034	0.273	85.9	317.0	3.0
1050	10	$130.1e^{-9}$	52.544	0.039	0.02231	0.00039	0.242	0.033	0.00889	0.00058	0.871	93.4	317.8	3.1
1100	10	$81.5e^{-9}$	51.397	0.081	0.01941	0.00130	0.005	0.050	0.00514	0.00105	0.020	98.2	317.6	3.5
1130	10	$32.2e^{-9}$	53.825	0.090	0.02535	0.00232	0.071	0.121	0.01561	0.00290	0.254	100.0	313.7	5.8
Biotite IV4-1, charge 45.37 mg, $J = 0.004731 \pm 0.000058$*; integral age = 268.3 ± 3.1 Ma; age of plateau (650–1050°C) = 269.2 ± 3.1 Ma														
550	10	$34.6e^{-9}$	35.910	0.049	0.02817	0.00020	0.004	0.123	0.02803	0.00103	0.013	1.4	221.6	3.5
650	10	$280.9e^{-9}$	35.134	0.010	0.01999	0.00015	0.004	0.015	0.00409	0.00019	0.013	13.3	268.5	3.1
700	10	$488.2e^{-9}$	34.338	0.006	0.01952	0.00009	0.026	0.008	0.00177	0.00008	0.095	34.4	267.7	3.1
750	10	$315.2e^{-9}$	34.248	0.009	0.01960	0.00017	0.005	0.019	0.00093	0.00015	0.017	48.1	268.9	3.1
800	10	$60.2e^{-9}$	35.033	0.018	0.01914	0.00051	0.053	0.089	0.00314	0.00068	0.190	50.6	269.9	3.4
875	10	$77.7e^{-9}$	35.242	0.026	0.01887	0.00051	0.081	0.063	0.00461	0.00025	0.292	53.9	268.2	3.1
950	10	$200.8e^{-9}$	34.660	0.006	0.01963	0.00015	0.003	0.013	0.00209	0.00012	0.012	62.5	269.4	3.1
1000	10	$472.9e^{-9}$	34.371	0.004	0.01925	0.00007	0.001	0.011	0.00134	0.00011	0.005	83.0	268.9	3.1
1025	10	$228.3e^{-9}$	34.536	0.008	0.01899	0.00024	0.031	0.014	0.00133	0.00019	0.111	92.8	270.1	3.1
1050	10	$107.1e^{-9}$	34.795	0.021	0.01853	0.00047	0.007	0.052	0.00178	0.00025	0.026	97.3	271.1	3.1
1130	10	$65.3e^{-9}$	36.595	0.017	0.02155	0.00046	0.300	0.062	0.00758	0.00077	1.080	100.0	271.7	3.5

* J means parameter characterizing neutron flux.

Table 3. Chemical analyses of three samples

Oxide, element	IV-4-1	604	139-1
SiO_2	70.23	73.03	68.17
Al_2O_3	15.41	15.01	16.01
TiO_2	0.56	0.24	0.54
$Fe_2O_{3\,tot}$	2.88	1.73	2.95
MnO	0.08	0.04	0.04
MgO	0.75	0.86	1.39
CaO	1.25	1.23	2.19
Na_2O	3.31	3.89	3.42
K_2O	3.37	3.06	4.58
P_2O_5	0.61	0.33	0.33
LOI	1.13	0.72	0.44
Total	99.60	100	100
Sc	2.99	2.55	6.65
V	22	13.4	39.5
Cr	13.2	13.1	18.2
Co	2.69	1.8	5.11
Ni	5.27	4	7.9
Rb	352	198	214
Sr	75.4	117	380
Y	12.4	6.52	18.6
Zr	257	87.6	201
Nb	11.2	5.64	10.3
Ba	311	322	1200
La	54.7	17.9	64.9
Ce	141	35.3	133
Pr	18.4	4.19	15.7
Nd	70.9	15.6	57.7
Sm	11	3.46	10.6
Eu	0.63	0.44	1.45
Gd	7.35	2.39	7.05
Tb	0.81	0.35	0.86
Dy	2.99	1.43	4.1
Ho	0.43	0.21	0.77
Er	1.13	0.49	1.72
Tm	0.17	0.08	0.2
Yb	0.93	0.70	1.33
Lu	0.13	0.09	0.24
Hf	7.46	2.35	5.74
Ta	1.73	0.98	1
Th	49.5	8.45	29.9
U	12.2	2.63	3.68

(CaO + MgO) · 5 plot (Fig. 7d) [5], their difference compared to A-type granites is clearly seen.

In the Rb–(Y + Nb) and Ta–Yb plots, where granitoids are divided by geodynamic settings (Fig. 8) [35], the data points of granitoids are localized in the boundary zone between fields of volcanic arcs and syncollision granites.

The initial $^{87}Sr/^{86}Sr$ ratios of granitoids range from 0.70416 to 0.70527 (Table 4), characteristic of island-arc I-type granites or granitoids of continental margins, which cut through accretionary island-arc crust [1, 27].

DISCUSSION

The studied massifs in the Northern Taimyr are composed of leucogranite and granite. The age of zircons crystallization in these massifs corresponds to the Early–Late Carboniferous (Visean–Bashkirian). Taking into consideration that the age of samples 604 and IV-4-1 is related only to the final phase of magmatic activity, the age of the master magmatic event may be several million years older. The dates obtained are markedly older than published earlier [2] and make it possible to refer the onset of granitoid magmatism in the Northern Taimyr to the Visean Age. This conclusion agrees with studies on reconstructing the sources of Carboniferous clastics, demonstrating that Taimyr–Severnaya Zemlya Fold Zone could have supplied clastic material to the northeastern margin of the Siberian Platform beginning from the Late Visean [7, 12, 20].

The petrographic and geochemical features of the studied granitoids make it possible to correlate them with differentiated I-type granites. Melanocratic I-type granites are so far unknown. An Andean-type continental margin is the most probable setting for the formation of high-K alkali–calc and calc–alkali granitoids of the I-type (including highly differentiated varieties) [37]. This is corroborated by the strontium isotopic composition of the studied granitoids ($^{87}Sr/^{86}Sr$ = 0.70416, 0.70459, 0.70527), which is characteristic of I-type granitoids [16, 19, 27, 36]; by their magnesian-type index Fe*; and by the minima of the Nb and Ta contents in spider diagrams. The data indicate that the active margin at the southern edge of the Kara Block started to evolve in the Early Carboniferous.

The $^{40}Ar/^{39}Ar$ ages of micas in the studied granitoids vary from the Early Carboniferous (sample 604) to the Middle Permian (samples 139-1, IV-4-1). The $^{40}Ar/^{39}Ar$ age of muscovite from sample 604 is close to the U–Pb zircon age within the uncertainty limits. This implies that granitoids crystallized at a small depth during the rapid cooling of magmatic bodies.

Note that there is a substantial difference in the ages obtained by the U–Pb method for zircons and the $^{40}Ar/^{39}Ar$ method for muscovite and biotite of samples 139-1 and IV-4-1. The difference in the crystallization temperature of certain minerals [23] makes it possible

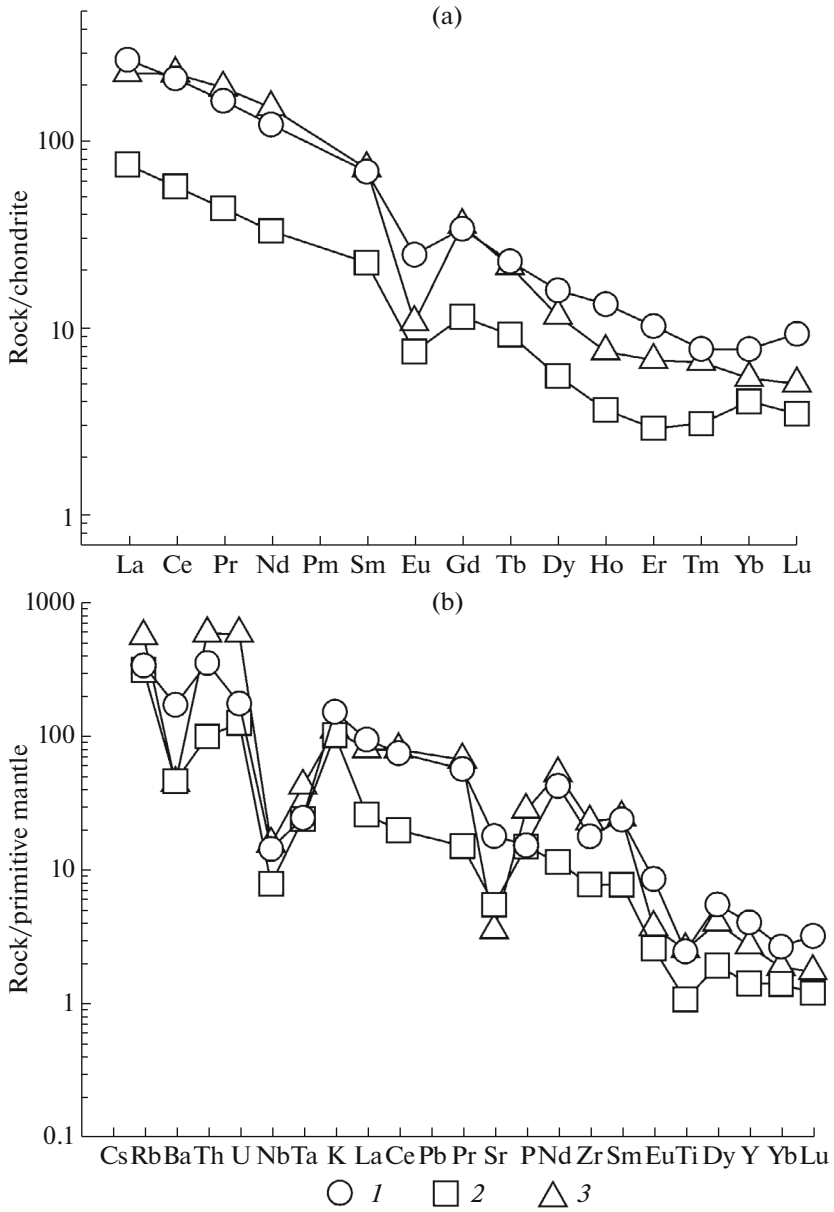

Fig. 6. (a) Chondrite- and (b) primitive mantle-normalized distributions of chemical elements in granitoids of Northern Taimyr. Chondrite and primitive mantle composition are taken from [32]. Numerals of samples: (*1*) 139-1, (*2*) 604, (*3*) IV-4-1.

to estimate the cooling rate of igneous complexes, the erosion rate of island arcs and active Andean-type continental margins [31, 38], and/or the age of metamorphism. For sample 139-1, the difference is ~75 and ~62 Ma for sample IV-4-1. According to various authors, the cooling rate of the granite massif varies widely [22, 24, 26], but the minimal rate does not drop below 20°C/Ma^{-1}. For sample IV-4-1, a rate of cooling is calculated at 11.5°C/Ma^{-1} and 7.5°C/Ma^{-1} for sample 139-1. The low cooling rate of the studied

Table 4. Results of determination of isotopic $^{87}Sr/^{86}Sr$ ratios

Sample	Age, Ma	$^{87}Rb/^{86}Sr$	$^{87}Sr/^{86}Sr$	Error ±	$(^{87}Sr/^{86}Sr)_i$
IV-4-1	321	13.34970	0.76515	0.000004	0.70416
139-1	315	1.57810	0.71167	0.000004	0.70459
604	344	5.08440	0.73017	0.000003	0.70527

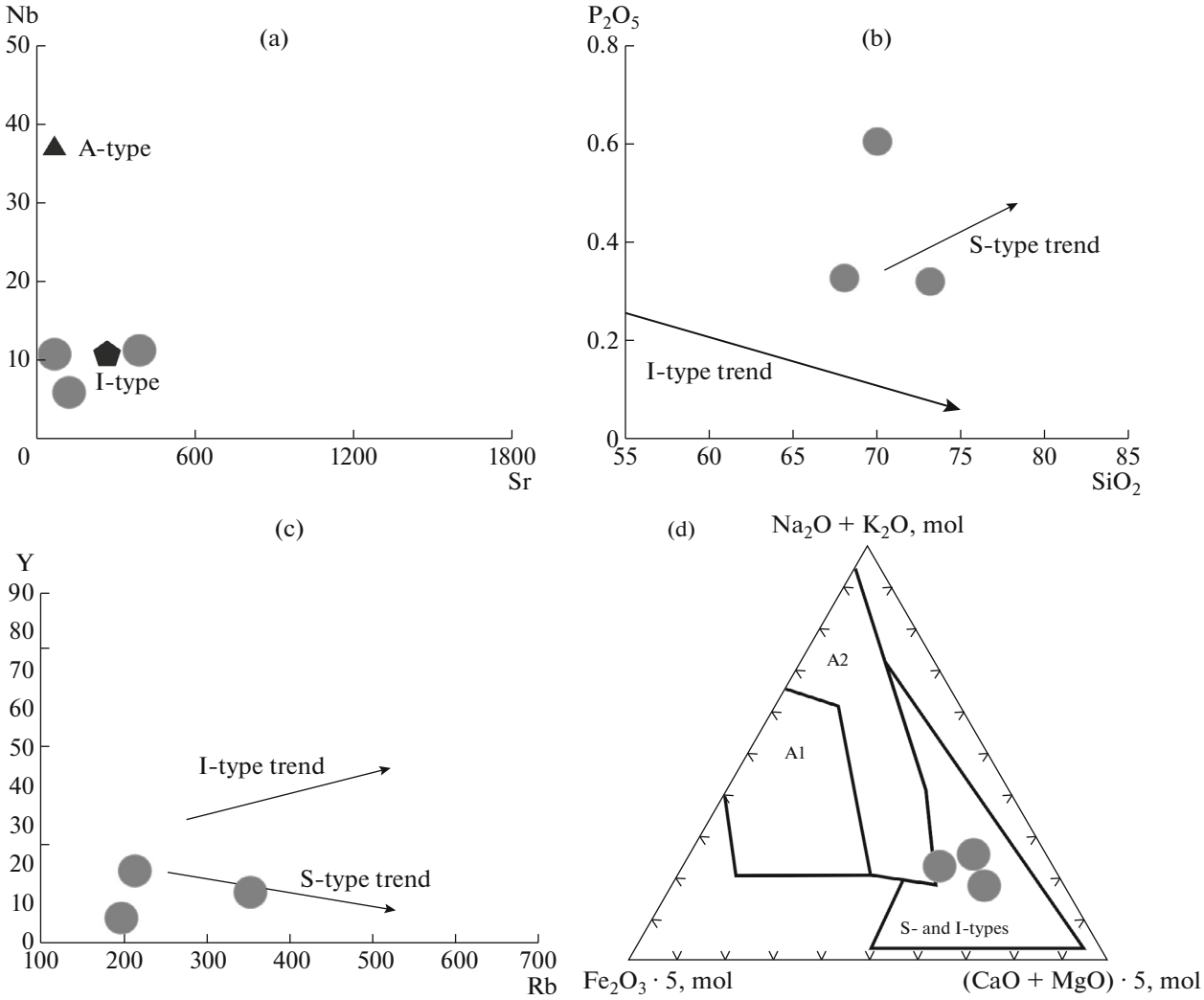

Fig. 7. Plots of chemical compositions of granitic rocks from Northern Taimyr: (a) Nb–Sr [39] (b) P_2O_5–SiO_2, (c) Y–Rb [18], $Fe_2O_3 \cdot 5$–$(Na_2O + K_2O)$–$(CaO + MgO) \cdot 5$ ($SiO_2 > 67\%$, molecular amounts), (d) for Northern Taimyr granitoids.

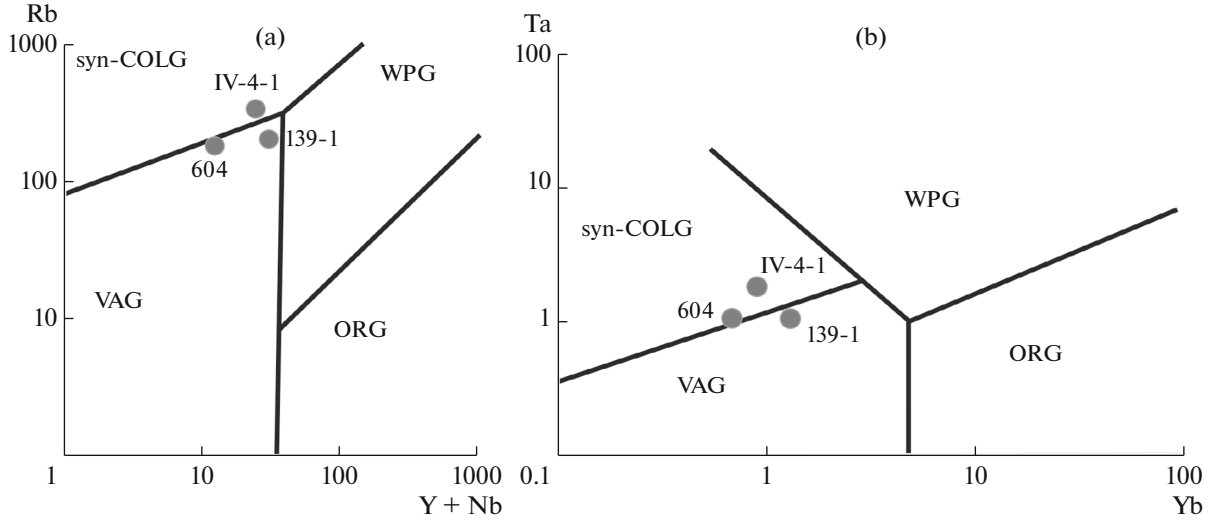

Fig. 8. Plots of chemical compositions of granitic rocks from Northern Taimyr: (a) Rb–(Y + Nb) and (b) Ta–Yb [35]. Fields of granites: syn-COLG, syncollision; VAG, volcanic arc granite; WPG, within-plate granite; OPG, oceanic ridge granite.

granitoids (taking into account that they are represented by relatively small massifs) allows the conclusion that the dates obtained by the $^{40}Ar/^{39}Ar$ method for samples 139-1 and IV-4-1 mark the repeated closure of the isotopic system as a result of a metamorphic event that occurred in the Permian.

Late Paleozoic magmatism in Arctic regions remains poorly studied, and this hinders the interpretation of its tectonic evolution. Nevertheless, granitoids close in age are known in several Arctic regions. Early Carboniferous (Tournaisian) granitoids that formed in a suprasubduction marginal continental setting have been described on the Chukchi Peninsula [10]. Occurrences of Late Devonian granitoids are also known there [34]. Luchitskaya et al. [34] compares Late Devonian and Tournaisian magmatism on the Chukchi Peninsula to the Ellesmere Orogeny developing in Arctic Canada [10]. The age of granitoids studied by us is Visean–Bashkirian, i.e., much younger than Tournaisian granitoids on the Chukchi Peninsula. This implies that the granitoid magmatism of the Northern Taimyr is hardly related to the Ellesmere Orogeny. According to the model proposed in [28], the North Kara Terrane, including the Northern Taimyr, was a continuation of the continent of Baltia in the Early and Middle Paleozoic. Along the eastern margin of Baltia (in present-day coordinates) there was a closure of the Ural paleoocean in the Carboniferous [9, 13]. The Early Carboniferous and Bashkirian Age are characterized by accretion in the Transural Zone of the Ural Fold System. This gave rise to the formation of a tonalite–granodiorite intrusive complex and vigorous suprasubduction volcanic activity in the eastern Urals. Transition to the collisional stage took place in the late Bashkirian time [9]. The studied granitoids of the Northern Taimyr are characterized by a suprasubduction nature, and the time of their formation is close to the known accretionary–collisional events in the Ural Orogen. This makes it possible to conclude that their emplacement is related to closure of the Ural ocean and the studied region is apparently a continuation of Baltia. The $^{40}Ar/^{39}Ar$ dating of micas has shown that the isotopic system resumed in the Middle Permian. Apparently, this event corresponds to an episode of regional metamorphism in the studied region, which is coeval with the final stages of collision of the Kara Terrane with Siberian continent and agree in general with paleomagnetic research data [11, 33].

CONCLUSIONS

(1) The Early–Middle Carboniferous age of granitoid massifs on the Northern Taimyr has been established.

(2) The studied granitoids are similar in geochemical and isotopic characteristics to fractionated I-type granites. This allows a conclusion on the suprasuduction (marginal continental) setting of their formation.

(3) The existence of an active margin in the Carboniferous along the southern edge of the Kara Block (in present-day coordinates) confirms the concept that the studied region was closely related to the continent of Baltia.

(4) Based on the results of $^{40}Ar/^{39}Ar$ dating of micas, a thermal event that led to resumption of the isotopic system took place in Middle Permian and was apparently related to regional metamorphism within the studied.

ACKNOWLEDGMENTS

Fieldwork and geochronological dating were performed in the framework of compiling the State Geological Map of Russian Federation on a scale of 1 : 1000000. Determination of the concentration of minor elements, Sr isotopic study, and processing and interpretation of isotopic data were supported by the Russian Science Foundation (project no. 17-17-01171).

REFERENCES

1. N. V. Andreeva and E. P. Izokh, *Intrusive Series of the Magadan Massif and Criteria of Their Identification* (SVKNII DVO AN SSSR, Magadan, 1990) [in Russian].
2. V. A. Vernikovskii, *Geodynamic Evolution of the Taimyr Folded Zone* (Sib. Otd. Ross. Akad. Nauk, Novosibirsk, 1996) [in Russian].
3. V. A. Vernikovsky, E. B. Sal'nikova, A. B. Kotov, V. A. Ponomarchuk, V. P. Kovach, V. A. Travin, S. Z. Yakovleva, and N. G. Berezhnaya, "The age of postcollisional granitoids of the northern Taimyr: U–Pb, Sm–Nd, Rb–Sr, and Ar–Ar Data," Dokl. Earth Sci. **363**, 1191–1194 (1998).
4. *State Geological Map of Russian Federation. Scale 1 : 1000000 (Third Generation). Sheet T-45–48, Cape Chelyuskin. Explanatory Note*, Ed. by A. A. Makar'ev (Kartfabrika VSEGEI, St. Petersburg, 2013) [in Russian].
5. A. V. Grebennikov, "*A*-type granites and related rocks: Petrogenesis and classification," Russ. Geol. Geophys. **55**, 1074–1086 (2014).
6. L. A. Daragan-Sushchova, O. V. Petrov, Yu. I. Daragan-Sushchov, and M. A. Vasil'ev, "Geological structure peculiarities of the North Kara shelf from seismic data," Reg. Geol. Metallog., No. 54, 5–16 (2013).
7. V. B. Ershova, A. K. Khudoley, and A. V. Prokopiev, "Reconstruction of provenances and Carboniferous tectonic events in the north-east Siberian Craton framework according to U–Pb dating of detrital zircons," Geotectonics **47**, 93–100 (2013).
8. L. P. Zonenshain, M. I. Kuz'min, and L. M. Natapov, *Plate Tectonics of the USSR Territory*, Vol. II (Nedra, Moscow, 1990) [in Russian].
9. K. C. Ivanov, V. A. Kontorovich, V. N. Puchkov, Yu. N. Fedorov, and Yu. V. Erokhin, "Tectonics of the

Urals and West Siberia basement: Main features of geological structure and evolution," Geol. Miner.-Syr'evye Resur. Sib., No. 2., 22–35 (2014).

10. M. V. Luchitskaya, S. D. Sokolov, A. B. Kotov, L. M. Natapov, E. A. Belousova, and S. M. Katkov, "Late Paleozoic granitic rocks of the Chukchi Peninsula: Composition and location in the structure of the Russian Arctic," Geotectonics **49**, 243–268 (2015).
11. D. B. Metelkin, V. A. Vernikovsky, and A. Yu. Kazansky, "Tectonic evolution of the Siberian paleocontinent from the Neoproterozoic to the Late Mesozoic: Paleomagnetic record and reconstructions," Russ. Geol. Geophys. **53**, 883–899 (2012).
12. A. V. Prokopiev, V. B. Ershova, E. L. Miller, and A. K. Khudoley, "Early Carboniferous paleogeography of the northern Verkhoyansk passive margin as derived from U–Pb dating of detrital zircons: Role of erosion products of the Central Asian and Taimyr–Severnaya Zemlya fold belts," Russ. Geol. Geophys. **54**, 1195–1204 (2013).
13. V. N. Puchkov, *Geology of the Urals and Cis-Uralian Region: Topical Problems of Stratigraphy, Tectonics, Geodynamics, and Metallogeny* (DizainPoligrafServis, Ufa, 2010) [in Russian].
14. V. M. Savatenkov, I. M. Morozova, and L. K. Levsky, "Behavior of the Sm–Nd, Rb–Sr, K–Ar, and U–Pb isotopic systems during alkaline metasomatism: Fenites in the outer-contact zone of ultramafic-alkaline intrusion," Geochem. Int. **42**, 899–920 (2004).
15. A. V. Travin, D. S. Yudin, A. G. Vladimirov, S. V. Khromykh, N. I. Volkova, A, Mekhonoshin, and T. B. Kolotilina, "Thermochronology of the Chernorud granulite zone, Ol'khon region, Western Baikal area," Geochem. Int. **47**, 1107–1124 (2009).
16. R. L. Armstrong, W. H. Taubeneck, and P. O. Hales, "Rb–Sr and K–Ar geochronometry of Mesozoic granitic rocks and their Sr isotopic composition, Oregon, Washington, and Idaho," Geol. Soc. Am. Bull. **88**, 397–411 (1977).
17. L. P. Black, S. L. Kamo, C. M. Allen, J. N. Heinikoff, D. W. Davis, J. Russel, R. J. Korsch, and C. Foudonlis, "TEMORA 1: A new zircon standard for U–Pb geochronology," Chem. Geol. **200**, 155–170 (2003).
18. B. W. Chappell and A. J. R. White, "I- and S-type granites in the Lachlan Fold Belt," Trans. R. Soc. Edinburgh: Earth Sci. **83**, 1–26 (1992).
19. B. W. Chappell and A. J. R. White, "Two contrasting granite types: 25 years later," Aust. J. Earth Sci. **48**, 489–500 (2001).
20. V. B. Ershova, A. V. Prokopiev, and A. K. Khudoley, "Integrated provenance analysis of Carboniferous deposits from Northeastern Siberia: Implication for the late Paleozoic history of the Arctic," J. Asian Earth Sci. **109**, 38–49 (2015).
21. B. R. Frost, C. G. Barnes, and W. J. Collins, "A geochemical classification for granitic rocks," J. Petrol. **42**, 2033–2048 (2001).
22. T. M. Harrison, I. Duncan, and I. McDougall, "Diffusion of ^{40}Ar in biotite – temperature, pressure, and compositional effects," Geochim. Cosmochim. Acta **49**, 2461–2468 (1985).
23. K. V. Hodges, "Geochronology and thermochronology in orogenic system," in *The Crust*, Vol. 3 of *Treatise on Geochemistry*, Ed. by H. D. Holland and K. K. Turekian (Elsevier, Oxford, 2004), pp. 263–292.
24. D. K. Holm and R. K. Dokka, "Interpretation and tectonic implications of cooling histories: An example from the Black Mountains, Death Valley extended terrane, California," Earth Planet. Sci. Lett. **116**, 63–80 (1993).
25. P. W. O. Hoskin and U. Schaltegger, "The composition of zircon and igneous and metamorphic petrogenesis," in *Zircon*, Vol. 53 of *Rev. Mineral. Geochem.*, Ed. by J. M. Hanchar and P. W. O. Hoskin (2003), pp. 27–62.
26. Å. Johansson, H. Maluski, and D. G. Gee, "Ar–Ar dating of Caledonian and Grenvillian rocks from northeasternmost Svalbard – Evidence of two stages of Caledonian tectonothermal activity in the high Arctic," Nor. Geol. Tidsskr. **81**, 263–281 (2001).
27. C. T. A. Lee, D. M. Morton, R. W. Kistler, and A. K. Baird, "Petrology and tectonics of Phanerozoic continent formation: From island arcs to accretion and continental arc magmatism," Earth. Planet. Sci. Lett. **263**, 370–387 (2007).
28. H. Lorenz, D. G. Gee, and A. Simonetti, "Detrital zircon ages and provenance of the Late Neoproterozoic and Palaeozoic successions on Severnaya Zemlya, Kara Shelf: A tie to Baltica," Norw. J. Geol. **88**, 235–258 (2008).
29. K. R. Ludwig, *SQUID 1.00, A User's Manual*, No. 2 of *Berkeley Geochronology Center Special Publication* (Berkeley Geochronol. Center, Berkeley, Calif., 2000).
30. K. R. Ludwig, *ISOPLOT 3.00. A User's Manual*, No. 4 of *Berkeley Geochronology Center Special Publication* (Berkeley Geochronol. Center, Berkeley, Calif., 2003).
31. J. Mao, Z. Li, X. Zhao, and J. Chin, "Geochemical characteristics, cooling history and mineralization significance of Zhangtiantang pluton in South Jiangxi Province, P.R. China," Chin. J. Geochem. **29**, 53–64 (2010).
32. W. F. McDonough and S. S. Sun, "Chemical and isotopic systematics of oceanic basalts: Implications for mantle composition and processes," in *Magmatism in the Ocean Basins*, Vol. 42 of *Geol. Soc. London, Spec. Publ.*, Ed. by A. D. Saunders and M. J. Norry (London, 1989), pp. 313–345.
33. D. V. Metelkin, V. A. Vernikovsky, A. Yu. Kazansky, O. K. Bogolepova, and A. P. Gubanov, "Paleozoic history of the Kara microcontinent and its relation to Siberia and Baltica: Paleomagnetism, paleogeography and tectonic," Tectonophysics **398**, 225–243 (2005).
34. B. Natal'in, J. M. Amato, J. Toro, and J. E. Wright, "Paleozoic rocks of northern Chukotka Peninsula, Russian Far East: Implications for the tectonic of Arctic region," Tectonics **18**, 977–1003 (1999).

35. J. A. Pearce, N. B. W. Harris, and A. G. Tindle, "Trace element discrimination diagrams for the tectonic interpretation of granitic rocks," J. Petrol. **25**, 956–983 (1984).

36. W. S. Pitcher, "The nature, ascent and emplacement of granitic magmas," J. Geol. Soc. (London, U. K.) **136**, 627–662 (1979).

37. T. W. Ruks, S. J. Piercey, J. J. Ryan, M. E. Villeneuve, and R. A. Creaser, "Mid- to late Paleozoic K-feldspar augen granitoids of the Yukon-Tanana terrane, Yukon, Canada: Implications for crustal growth and tectonic evolution of the northern Cordillera," Geol. Soc. Am. Bull. **118**, 1212–1231 (2006).

38. T. E. Waight, D. Frei, and M. Storey, "Geochronological constraints on granitic magmatism, deformation, cooling and uplift on Bornholm, Denmark," Bull. Geol. Soc. Den. **60**, 23–46 (2012).

39. J. B. Whalen, K. L. Currie, and B. W. Chappell, "A-type granites: Geochemical characteristics, discrimination and petrogenesis," Contrib. Mineral. Petrol. **95**, 407–419 (1987).

40. I. S. Williams, "U–Th–Pb geochronology by ion microprobe: Applications of microanalytical techniques to understanding mineralizing processes," Rev. Econ. Geol. **7**, 1–35 (1998).

Reviewer: A.A. Shchipanskii

Translated by V. Popov